Buckling of superconducting structures : a variational approach using the law of Biot and Savart

EINDHOVEN UNIVERSITY OF TECHNOLOGY
Department of Mathematics and Computing Science

RANA 91-11
December 1991

BUCKLING OF SUPERCONDUCTING STRUCTURES. A VARIATIONAL APPROACH USING THE LAW OF BIOT AND SAVART

by
A.A.F. van de Ven
L.G.F.C. van Bree

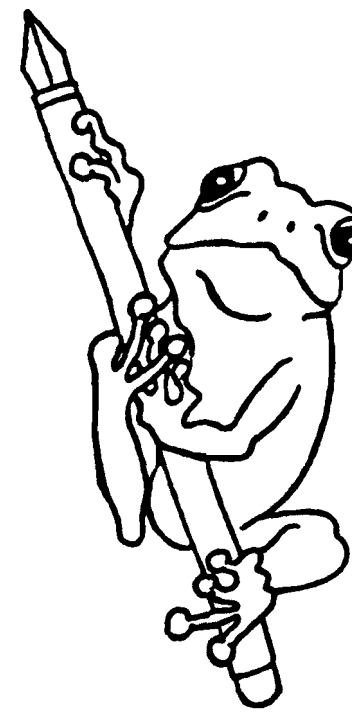

ISSN: 0926-4507
Reports on Applied and Numerical Analysis
Department of Mathematics and Computing Science
Eindhoven University of Technology
P.O. Box 513
5600 MB Eindhoven
The Netherlands

BUCKLING OF SUPERCONDUCTING STRUCTURES. A VARIATIONAL APPROACH USING THE LAW OF BIOT AND SAVART

A.A.F. van de Ven and L.G.F.C. van Bree

Department of Mathematics and Computing Science, Eindhoven University of Technology, P.O. Box 513, 5600 MB Eindhoven, The Netherlands

ABSTRACT

A structure of superconducting coils can collapse, due to the Lorentz forces acting between the members of the structure, whenever the electric current through the structure exceeds a certain critical value, the so called buckling current. A method is presented based upon a variational principle, which uses as admissible fields those derived from the Biot-Savart law. This method combines the mathematical exactness of the variational principle with the straightforward availability of the Biot-Savart fields. Applications are presented for sets of n parallel rods ($n \geq 2$) and for (finite or infinite) helical and spiral coils. For all these cases the buckling current is calculated and, moreover, some information about the buckling modes is provided. These buckling currents and modes are most easily found by using sinusoidal series representations for the buckling displacements. In all applications it is assumed that we deal with slender systems; the precise criterion for this is presented for each specific system. It turns out that for all systems considered in this paper the formula for the buckling current is globally the same; only a pre-factor differs in each case.

1. Introduction

In this paper we shall consider superconducting slender (beam-like) bodies, or systems of such bodies, carrying a prescribed current I_0. The system is placed in a vacuum. The magnetic field in the vacuum is solely due to the own field of the conductors generated by the current I_0. The Lorentz forces which are due to the interaction of this magnetic field with the current I_0 can cause the structural system to become unstable. We call this magnetoelastic buckling and the critical value of the current I_0 for which the system becomes unstable is called the buckling current.

The research on magnetoelastic buckling as started by F.C. Moon was in first instance focussed on the buckling of soft ferromagnetic beams or plates (cf. for instance [1]). In later years from a technical point more important subject of magnetoelastic stability of superconducting structures came into view. For an excellent review of magnetoelastic buckling problems see the monograph of F.C. Moon [2]. Moon, in cooperation with S. Chattopadhyay, reported on the buckling and vibration of structures (such as rods or rings) carrying electric current already in 1975 (cf. [3] and [4]). The magnetoelastic stability of a superconducting ring in its own field was investigated by Van de Ven and Couwenberg, [5] (who proved that this system was always stable). In recent years a lot of papers on the buckling of superconducting structures has appeared, but we confine ourselves here to mentioning only the work of Miya *et al.* [6], [7] and of Geiger and Jüngst, [8] (these works are more specifically directed to technologically relevant solutions than the present one, whose first object it is to built a firm theoretical basis). For a more complete list of references we refer to [2].

In a series of papers, [9]–[12], the first author together with his coworkers Van Lieshout, Rongen and Smits, presented a variational principle that could be applied to magnetoelastic buckling problems for both soft ferromagnetic as well as superconducting structures. This method was based upon a chosen expression for the Lagrangian for a soft magnetic or superconducting body in vacuum. This Lagrangian was developed up to the second order in perturbations which are due to the buckling displacements of the body. From the thus obtained second variation an explicit expression for the buckling current was derived. This method was presented in [9], whereas in [10], [11] and [12] applications are given to sets of superconducting rods or rings. In [10]–[12] also a second more direct method was presented. This method starts from a formula for the Lorentz force on a current carrier derived from the Biot-Savart law (cf. [2], Sect. 2.6). Therefore, we refer to this method as the Biot-Savart method. The second method is less exact than the first one, but much easier to work with in practice. A comparison of the results of both methods showed a reasonable agreement.

In this respect, it seems profitable to use to look for a method that combines the advantages of the two methods mentioned above, i.e. the greater exactness of the variational method and the convenience for the user pertinent to the Biot-Savart method. To this end we shall use in the variational formulation of the first method an admissable field obtained on base of the Biot-Savart law. Our expectation that this combined approach will yield a useful approximation for the buckling current is supported by the observed correspondence between the results of the two respective methods.

In Section 3 the details of this combined method will be presented. However, before doing so, we shall give in Section 2 short descriptions of the variational method and the Biot-Savart

method. Moreover, we shall list the main results obtained by these two methods thusfar. A comparison of the results leads us to the conclusion that, firstly, the differences in the results of the two methods are small (under certain conditions) and that, secondly, certain simplifications in the model are admissable. The specific nature of these simplifications and the restrictions under which they are allowable will be given in Section 2.

The combined approach of Section 3 together with the simplifications of Section 2 results in a method for the calculation of buckling currents of (more or less) complex structures that is on one hand sufficiently precize (provided certain explicit given conditions are fulfilled) and on the other convenient in applications. As an illustration of the combined method we shall in Section 4 reconsider the buckling problem of two parallel superconducting rods (this problem was earlier treated in [10], and solved there by means of the two basical methods). The obtained result could easily be generalized to an arbitrary number (n) of rods ($n \geq 2$, including $n \to \infty$). One of the results of this section turned out to be directly applicable to the more complex problems dealt with in the Sections 5 and 6.

In Section 5 we shall apply the combined method to two types of cylindrical helical conductors. We shall consider, firstly, an infinitely long superconductor in the form of a cylindrical helix, periodically supported in equidistant points and, secondly, a finite helix (n turns) supported in its end points. As a second example, in Section 6 we shall investigate the buckling problem for a conductor wound in the form of a flat spiral. For both examples we shall calculate by numerical means a set of values for the buckling current as a function of the system parameters (e.g. the number of coils n). It turns out that for all the systems considered here the formula for the buckling current has essentially the same basic form. Moreover we succeeded in finding a pair of empirical formulas, very simple of nature, giving directly the buckling value for a helical or a spiral conductor.

2. Description of the two basic methods and earlier results

We start by giving in main lines a description of our variational method for a superconducting body in vacuum. Essential in our model for a superconductor is the assumption that the current runs over the surface of the superconductor only, thus shielding the body from a magnetic field. Hence, there is no internal magnetic field inside the body. The magnetic field in the vacuum surrounding the body is denoted by $\mathbf{B}$ and has to satisfy Ampère's law ($\mu_0 = 4\pi \times 10^{-7}$)

$$\int_C (\mathbf{B},\mathbf{t})\, ds = \mu_0 I_0 \ , \tag{2.1}$$

where C is a contour entirely in the vacuum, encircling the current carrier, while $\mathbf{t}$ is the unit tangent vector at C. Moreover, I_0 is the prescribed total current through the current carrier.

Our variational method is based upon a chosen expression for the Lagrangian for an elastic superconducting body which in this case reads (cf. [11], (2.4), or [13], (2))

$$L = -\int_{G^-} \rho U \, dV + \frac{1}{2\mu_0} \int_{G^+} (\mathbf{B},\mathbf{B})\, dV \ , \tag{2.2}$$

where the first integral represents the elastic energy of the deformed body (ρU is the elastic energy density) and the second one is the magnetic energy of the vacuum field. Note that in (2.2) G^- and G^+ are the configurations of the body and the vacuum, respectively, *in the deformed state.*
Variation of (2.2) with respect to $\mathbf{B}$ and to the displacement $\mathbf{u}$ under the constraints (2.1) and

$$\operatorname{curl} \mathbf{B} = \mathbf{0} \ , \quad \mathbf{x} \in G^+ \ ; \ \mathbf{B} \to \mathbf{0} \ , \ |\mathbf{x}| \to \infty \ , \tag{2.3}$$

leads to the common 3-dimensional model of magnetoelastic interactions (see e.g. [14]). In this model the electromagnetic forces are Lorentz forces acting at the surface of the body. These forces cause a deformation of the body. For stability considerations we have to distinguish between two different equilibrium states of the body, i.e. (i) the intermediate state and (ii) the final (or buckled) state. Since in the intermediate state the deformations are small (and in first approximation irrelevant for the determination of the buckling point) we may approximate this state by the rigid-body state. The only unknown then is the rigid-body field $\mathbf{B}_0$. In the final state the unknowns are the displacement $\mathbf{u}$ and the magnetic field $\mathbf{B}$. The latter is written as

$$\mathbf{B} = \mathbf{B}_0 + \mathbf{b} \ , \tag{2.4}$$

so $\mathbf{b}$ is the perturbation of the external magnetic field due to the buckling deflection of the body.

In [11] (in analogy with [9]) the Lagrangian (2.2) is developed up to the second order in the perturbations $\mathbf{u}$ and $\mathbf{b}$. Thus, the variation of L with respect to these variables can be written as

$$L - L^{(0)} = \delta L + \tfrac{1}{2}\,\delta^2 L + \dots \ . \tag{2.5}$$

Since the intermediate state is an equilibrium state the first variation of L must be zero, so

$$\delta L = 0 \ , \tag{2.6}$$

and

$$L - L^{(0)} = \tfrac{1}{2}\,\delta^2 L =: J(\mathbf{b}, \mathbf{u}) \ , \tag{2.7}$$

where J is a homogeneously quadratic functional in the perturbations. The final state is an equilibrium state and, therefore, the first variation of J must be zero, i.e.

$$\delta J(\mathbf{b}, \mathbf{u}) = 0 \ . \tag{2.8}$$

In what follows we shall choose admissable fields for $\mathbf{B}_0$ and $\mathbf{b}$ and, thereafter, we shall equate the first variation of J with respect to $\mathbf{u}$ equal to zero. This yields a linear eigenvalue problem for I_0^2 from which the buckling value I_0 can be obtained.

For the examples considered in [10], [11] and [12], however, we were able to calculate the *exact* fields $\mathbf{B}_0$ and $\mathbf{b}$, thus obtaining exact values for the buckling current I_0. In these papers the following systems were investigated

i) two parallel rods, distance 2a, support length l (see also Sect. 4),

ii) two concentric (coplanar) rings, radii $b_1 = b + a$, $b_2 = b - a$,

iii) two coaxial rings, distance $2a$, radii $b_1 = b_2 = b$,

iv) a set of n parallel rods (for $n = 3, 4, 5$), distances $2a$, support length l.

In all these examples the cross-section of the current carrier (rod or ring) is circular, radius R. Moreover, all systems are assumed to be slender, meaning that

$$R < a \ll l \ , \tag{2.9}$$

where l must be replaced by πb for the cases ii) and iii).
The resulting buckling values are listed in the first column of Table 1. There, E is Young's modulus, ν is Poisson's modulus and Q is a numerical factor depending on a/R only (cf. [10], Table 4).

The second method is based upon a generalisation of the law of Biot and Savart as is described by Moon in [2], Sect. 2.6. Let $\mathbf{B}(\mathbf{x})$ be the magnetic field in a point $\mathbf{x} \in G^+$ created by an electric circuit $\mathcal{L}$ to be considered as a one-dimensional curve. Then (cf. [2], Eq. (2-6.3))

$$\mathbf{B}(\mathbf{x}) = \frac{\mu_0 I_0}{4\pi} \int_{\mathcal{L}} \frac{\mathbf{t}(s) \times \mathbf{R}(s, \mathbf{x})}{R^3(s, \mathbf{x})}\, ds \ , \tag{2.10}$$

where $\mathbf{t}(s)$ is the unit tangent vector on $\mathcal{L}$ in a point P on $\mathcal{L}$ having arc length s, and $\mathbf{R}(s,\mathbf{x})$ is the position vector of the point $\mathbf{x}$ with respect to $P(R = |\mathbf{R}|)$.

In a way as suggested by Moon this formula can be used for the determination of the Lorentz force $\mathbf{F}$ in a point on one circuit due to another circuit. The thus obtained expression is linearized with respect to the displacements. The linear part of $\mathbf{F}$ serves as a load parameter in for instance a beam or a ring equation. That value for the current through the circuits for which the equation mentioned above has a non- trivial solution is the looked for buckling value I_0. We refer to this more direct method as the *Biot-Savart method.* More details of this method are given in [10], [11] and [12], where we have applied this method to the same examples as we did for the variational method (plus the case $n = \infty$ for example iv)). The results are listed in the second column of Table 1. We conclude that:

Table 1.

Buckling currents from the variational method ($I_0^{(V)}$) and the Biot-Savart method ($I_0^{(B)}$) for sets of (i) two parallel rods, (ii) two concentric rings, (iii) two coaxial rings, and (iv) n parallel rods ($n = 3,4,5,\infty$). (E is Young's modulus, ν is Poisson's modulus and Q is a numerical factor depending on a/R only (cf. [10], Table 4.))

		$I_0^{(V)}$	$I_0^{(B)}$
(i)		$\frac{\pi^3 R^3}{l^2}\sqrt{\frac{E}{\mu_0 Q}}$	$\frac{\pi^3 a R^2}{l^2}\sqrt{\frac{E}{\mu_0}}$
(ii)		$\frac{3\pi R^3}{b^2}\sqrt{\frac{E}{\mu_0 Q}}$	$\frac{3\pi a R^2}{b^2}\sqrt{\frac{E}{\mu_0}}$
(iii)		$\frac{6\pi R^3}{\sqrt{5+\nu}\,b^2}\sqrt{\frac{E}{\mu_0 Q}}$	$\frac{6\pi a R^2}{\sqrt{5+\nu}\,b^2}\sqrt{\frac{E}{\mu_0}}$
(iv)	$n = 3$	$\sqrt{\frac{2}{3}}\,\frac{\pi^3 R^3}{l^2}\sqrt{\frac{E}{\mu_0 Q}}$	$\sqrt{\frac{2}{3}}\,\frac{\pi^3 a R^2}{l^2}\sqrt{\frac{E}{\mu_0}}$
	$n = 4$	$0.753\,\frac{\pi^3 R^3}{l^2}\sqrt{\frac{E}{\mu_0 Q}}$	$0.753\,\frac{\pi^3 a R^2}{l^2}\sqrt{\frac{E}{\mu_0}}$
	$n = 5$	$0.723\,\frac{\pi^3 R^3}{l^2}\sqrt{\frac{E}{\mu_0 Q}}$	$0.723\,\frac{\pi^3 a R^2}{l^2}\sqrt{\frac{E}{\mu_0}}$
	$n = \infty$	$\frac{2\pi^2 R^3}{l^2}\sqrt{\frac{E}{\mu_0 Q}}$	$\frac{2\pi^2 a R^2}{l^2}\sqrt{\frac{E}{\mu_0}}$

1. The results per column only differ in a fixed factor, independent of a, R or $l(b)$. This

factor is solely due to the different elastic energies of the systems; the integral K takes for all these systems the same value (at least if we replace l by πb for the ring-systems). Since K is the same for a slender system of two rings as for a set of two rods, one may for the evaluation of the magnetic interaction between two rings replace these rings locally by two straight lines. This is exactly what is actually done in the Biot-Savart-method.

2. The results of the variational and the Biot-Savart-method differ from each other only in a factor

$$\frac{a}{R}\sqrt{Q}\,.$$

Hence, the results of both methods should be in agreement if

$$\frac{1}{\sqrt{Q}} = \frac{a}{R}\,. \tag{2.11}$$

It turns out ([10], Table 4) that for (a/R) not too close to unity the difference between $Q^{-1/2}$ and (a/R) is small and decreases with increasing (a/R) (e.g. for $a/R \geq 4$, the relative difference is less than 5%).

We claim that, once our model of a superconducting body is accepted, our variational theory is mathematically exact for slender systems (i.e. in the limit $a/l \to 0$). The Biot-Savart method is not exact in that, firstly, the three-dimensional current carrying bodies are considered as one-dimensional curves and, secondly, the force due to the self field of the conductor is neglected. The second point is not so important as our variational method shows that this self-effect is an $O(a^2/l^2)$-effect and, hence, negligible for slender systems. Due to the first point the specific shape of the cross-section and the distribution of the current over the cross-section are disregarded. It is precisely this aspect that causes the differences between the variational and the Biot-Savart-method. Since these differences are small for systems the members of which are not too close to each other (i.e. a/R not too close to 1) we conclude that in these cases the precise distribution of the current over the cross-section is not a question of the utmost importance.

3. The combined method

In this section we shall formulate our variational principle explicitly, in the form according to [11], and we shall use in this principle as an admissible field the one we shall obtain from the Biot-Savart law as given in (2.10).

According to [11], (2.22) (with $\Delta\psi = \psi_{,ii} = 0$, see (2.23)) the functional J takes the form (in the original, i.e. not-normalized, variables and with $\mathbf{B} = \mathbf{B_0}$)

$$J = \tfrac{1}{2} \int\limits_{G^-} \left[T_{jk}\, u_{i,jk}\, u_i - \frac{E}{1+\nu} \left(\frac{\nu}{1-2\nu}\, e_{kk}\, e_{ll} + e_{kl}\, e_{kl} \right) \right] dV$$

$$- \frac{1}{2\mu_0} \int\limits_{\delta G} \left[(\psi + B_k\, u_k)_{,j}\; B_j\, u_i + \frac{1}{2}\, B_k\, B_k (u_{j,j}\, u_i - u_{i,j}\, u_j - u_{j,i}\, u_j) \right.$$

$$\left. - \tfrac{1}{2}\, B_j\, B_k (u_{j,k} + u_{k,j})\, u_i + (\psi_{,i} + B_{i,j}\, u_j - B_j\, u_{i,j})\, \psi \right] N_i\, dS \; . \tag{3.1}$$

Here, $\mathbf{B}$ is the rigid-body field, ψ the perturbed magnetic potential, i.e.

$$\psi_{,i} = b_i \; , \tag{3.2}$$

E and ν are Young's and Poisson's modulus, respectively, T_{ij} are the pré-stresses (i.e. the stresses before buckling) and e_{ij} the linear deformations, i.e.

$$e_{ij} = \tfrac{1}{2} (u_{i,j} + u_{j,i}) \; . \tag{3.3}$$

Furthermore, G^- and ∂G are the original *undeformed* configuration of the body and its boundary, respectively, and $\mathbf{N}$ is the unit outward normal on ∂G.

In [11], as well as in [10] and [12], we used in (3.1) the exact solutions for $\mathbf{B}$ and ψ. However, if the systems become more complex it will become increasingly difficult (not to say impossible) to determine these fields exactly. Therefore, we note that $\delta J = 0$ for variations of $\mathbf{B}$, ψ and $\mathbf{u}$ satisfying the following sets of constraints:

i) (2.1) and (2.3).

ii) $$\Delta\psi = \psi_{,ii} = 0 \; , \quad \mathbf{x} \in G^+ \; ; \quad \psi \to 0 \; , \quad |\mathbf{x}| \to \infty \; . \tag{3.4}$$

Fields $\mathbf{B}(\mathbf{x})$ and $\psi(\mathbf{x})$ which satisfy these constraints are called admissible fields.

If we can find admissible fields for $\mathbf{B}$ and ψ that are not too far away from the exact fields, we can use these fields in (3.1) to obtain an approximation for J. Here, we shall use the Biot-Savart fields as they can be derived from (2.10). We shall show that these fields are admissible. The good correspondence between the results of the variational method and the Biot-Savart method as found in the preceding section, supports us in our opinion that the

above choice leads to useful admissible fields and to a good approximation of the buckling current.

Before proceeding with the explicit derivation of the admissible fields, we first simplify the expression (3.1). To this end, we realize that we wish to apply (3.1) to the buckling of slender (beam-like) bodies. In this kind of buckling the pure deformations are much smaller than the local rotations of the body. This brings us to neglect in the magnetic term in (3.1) (i.e. the second integral on the right-hand side of (3.1)) those terms that contain a factor of the order $B^2 \, \|e_{ij}\|$ (in fact the second and third term). Since, moreover, the term with the pré-stresses T_{ij} occurring in the first integral is of the same order, this term can be neglected too. We like to mention that, as is shown in [10] and [11], the neglect of the above terms leads to an error of the order (R/l) and, hence, is justified for systems of slender bodies. Alltogether this leads us to the following simplified expression for J

$$J = -\frac{E}{2(1+\nu)} \int\limits_{G-} \left[\frac{\nu}{1-2\nu} \, e_{kk} \, e_{ll} + e_{kl} \, e_{kl}\right] dV$$

$$-\frac{1}{2\mu_0} \int\limits_{\partial G} \left[(\psi + B_k \, u_k)_{,j} \, B_j \, u_i + (\psi_{,i} + B_{i,j} \, u_j - B_j \, u_{i,j}) \, \psi\right] N_i \, dS$$

$$= -W + I_0^2 \, K \; . \tag{3.5}$$

We have written the last term in (3.5) as $I_0^2 \, K$, because K is independent of I_0 then. This is due to the fact that $\mathbf{B}$ and ψ are linear in I_0.

With $B_{i,j} = B_{j,i}$ (as follows from $(2.3)^1$) we can reduce the integral $I_0^2 \, K$ as given by (3.5) still somewhat more to obtain

$$I_0^2 \, K = -\frac{1}{2\mu_0} \int\limits_{\partial G} \left[(\psi + B_k \, u_k)_{,j} \, (B_j \, u_i \, N_i + \psi \, N_j)\right] dS \; , \tag{3.6}$$

where we have neglected again a term proportional to $B^2 \, \|e_{ij}\|$.

It is possible to derive explicit expressions for admissible $\mathbf{B}(\mathbf{x})$ and $\psi(\mathbf{x})$ from (2.10) for arbitrary (curved) circuits, but we shall refrain from doing so here. The results of Sect. 2, especially conclusion 1, learned us that for the determination of the above K- integral it suffices to calculate its value for an interaction between two straight rods. This value for K can then also be used for systems of curved beams, such as a pair of rings, but also for helical or spiral conductors as we shall show in due course of this paper, provided this system satisfies the condition of slenderness (2.9). In this paper we shall restrict ourselves to such systems. Hence, we only need to calculate $\mathbf{B}$ and ψ for a straight current carrier $\mathcal{L}$, as we shall do now first.

Consider an infinite one-dimensional current carrier $\mathcal{L}$, carrying a current I_0. In the original state $\mathcal{L}$ forms a straight line along the $\mathbf{e}_3$-axis and a point P of $\mathcal{L}$ on this line is given by its position vector $\boldsymbol{\xi} = \zeta \, \mathbf{e}_3$.

The rigid-body field $\mathbf{B}(\mathbf{x})$ in an arbitrary point $\mathbf{x} \in G^+$, with $\mathbf{x} = x\,\mathbf{e}_1 + y\,\mathbf{e}_2 + z\,\mathbf{e}_3$, follows then from (2.10) as

$$\mathbf{B}(\mathbf{x}) = \frac{\mu_0 I_0}{4\pi} \int_{-\infty}^{\infty} \frac{\mathbf{e}_3 \times (\mathbf{x} - \boldsymbol{\xi})}{|\mathbf{x} - \boldsymbol{\xi}|^{3/2}}\, d\zeta =$$

$$= \frac{\mu_0 I_0}{4\pi} (x\mathbf{e}_2 - y\mathbf{e}_1) \int_{-\infty}^{\infty} \frac{d\zeta}{[x^2 + y^2 + (z-\zeta)^2]^{3/2}} =$$

$$= -\frac{\mu_0 I_0}{2\pi} \frac{(y\mathbf{e}_1 - x\mathbf{e}_2)}{(x^2 + y^2)} \,. \tag{3.7}$$

Clearly this field satisfies the constraints (2.1) and (2.3).

For the calculation of $\psi(\mathbf{x})$ we assume that the rod $\mathcal{L}$ has a normal deflection in the $\mathbf{e}_1$-direction, i.e.

$$\mathbf{u} = u(\zeta)\,\mathbf{e}_1 \,. \tag{3.8}$$

Then,

$$\mathbf{t} = u'\,\mathbf{e}_1 + \mathbf{e}_3 \,, \quad \left({}' = \frac{d}{d\zeta} \right) , \tag{3.9.1}$$

$$\mathbf{R} = (x - u)\,\mathbf{e}_1 + y\,\mathbf{e}_2 + (z - \zeta)\,\mathbf{e}_3 \,, \tag{3.9.2}$$

and (up to the first order in u)

$$R^{-3} = R_0^{-3}\left(1 + \frac{3x}{R_0^2}\,u\right) , \quad (R_0 = [x^2 + y^2 + (z-\zeta)^2]^{1/2}) \,, \tag{3.9.3}$$

and with this (2.10) yields for the perturbed field in $\mathbf{x} \in G^+$,

$$\mathbf{b}(\mathbf{x}) = \frac{\mu_0 I_0}{4\pi} \int_{-\infty}^{\infty} \frac{1}{R_0^3} \left[\frac{3x}{R_0^2} (x\mathbf{e}_2 - y\mathbf{e}_1)\, u(\zeta) - \{(z-\zeta)\,\mathbf{e}_2 - y\mathbf{e}_3\}\, u'(\zeta) - u(\zeta)\,\mathbf{e}_2 \right] d\zeta =$$

$$= -\frac{\mu_0 I_0}{4\pi} \left[3xy \int_{-\infty}^{\infty} \frac{u(\zeta)}{R_0^5}\, d\zeta \cdot \mathbf{e}_1 \right.$$

$$\left. + \int_{-\infty}^{\infty} \frac{1}{R_0^3} \left\{ u(\zeta) + (z-\zeta)\, u'(\zeta) - \frac{3x^2}{R_0^2}\, u(\zeta) \right\} d\zeta \cdot \mathbf{e}_2 - y \int_{-\infty}^{\infty} \frac{u'(\zeta)}{R_0^3}\, d\zeta \cdot \mathbf{e}_3 \right] =$$

$$= -\frac{\mu_0 I_0}{4\pi} \int_{-\infty}^{\infty} \left[\frac{3xy}{R_0^5}\, \mathbf{e}_1 - \left(\frac{1}{R_0^3} - \frac{3y^2}{R_0^5} \right) \mathbf{e}_2 + \frac{3y(z-\zeta)}{R_0^5}\, \mathbf{e}_3 \right] u(\zeta)\, d\zeta \,, \tag{3.10}$$

where the latter step follows after partial integration.
From (3.10) it follows that curl $\mathbf{b}(\mathbf{x}) = \mathbf{0}$ and, hence, there exists a potential $\psi(\mathbf{x})$ such that

$$\mathbf{b}(\mathbf{x}) = \operatorname{grad} \psi(\mathbf{x}) \,, \tag{3.11}$$

and this potential is equal to

$$\psi(\mathbf{x}) = \frac{\mu_0 I_0}{4\pi} \int_{-\infty}^{\infty} \frac{y\, u(\zeta)}{R_0^3}\, d\zeta \,. \tag{3.12}$$

It is easily checked that $\Delta\psi(\mathbf{x}) = 0$ and $\psi(\mathbf{x}) \to 0$ for $|\mathbf{x}| \to \infty$ so this result indeed satisfies the constraints (3.4).

We assume that the current carrier $\mathcal{L}$ is periodically supported over distances l. In that case $u(z) = 0$ in all points $z = \pm kl$, $k \in I\!N$, and, moreover, $u(z)$ is a periodic function of z with period $2l$. We now can write (3.12) as

$$\psi(\mathbf{x}) = \frac{\mu_0 I_0}{4\pi}\, y \left[u(z) \int_{-\infty}^{\infty} \frac{d\zeta}{R_0^3} + \int_{-\infty}^{\infty} \frac{u(\zeta) - u(z)}{R_0^3}\, d\zeta \right] =$$

$$= \frac{\mu_0 I_0}{4\pi} \cdot \frac{2y}{(x^2+y^2)}\, u(z) \left[1 + O\left(\frac{R^2}{l^2} \ln \frac{R}{l} \right) \right] . \tag{3.13}$$

In the latter step we have used the mean value theorem and we have assumed that for $\mathbf{x} \downarrow \partial G$ x and y are such that $(x^2+y^2)/l^2 = O(R^2/l^2)$ (in all our applications the latter condition is fulfilled). We note that with ψ according to (3.13) the constraint $\Delta\psi = 0$ is only satisfied up to an order (R^2/l^2)-term; to see this we have to introduce the non-dimensional coordinates $\hat{x} = x/R$, $\hat{y} = y/R$, $\hat{z} = z/l$.

In the next section we shall use the above result for the solution of the buckling problem of a set of two parallel straight rods. The solution of this problem is already known from [10], but we nevertheless treat this example first for three reasons:

1. as an illustration of the method proposed in this section;
2. because, and this is the most important reason, one of the results of this example, namely the value of the integral K, can directly be applied to more complex problems such as those that will be treated in Sections 5 and 6;
3. in order to show that the combined method leads to a solution that is even closer to the result of the variational method than the Biot- Savart result itself.

4. A set of two parallel rods

Consider two straight conductors $\mathcal{L}_1$ and $\mathcal{L}_2$, both carrying a current I_0. The conductors are infinitely long and periodically supported over length l. A cross-sectional view of the set is drawn in Figure 1.

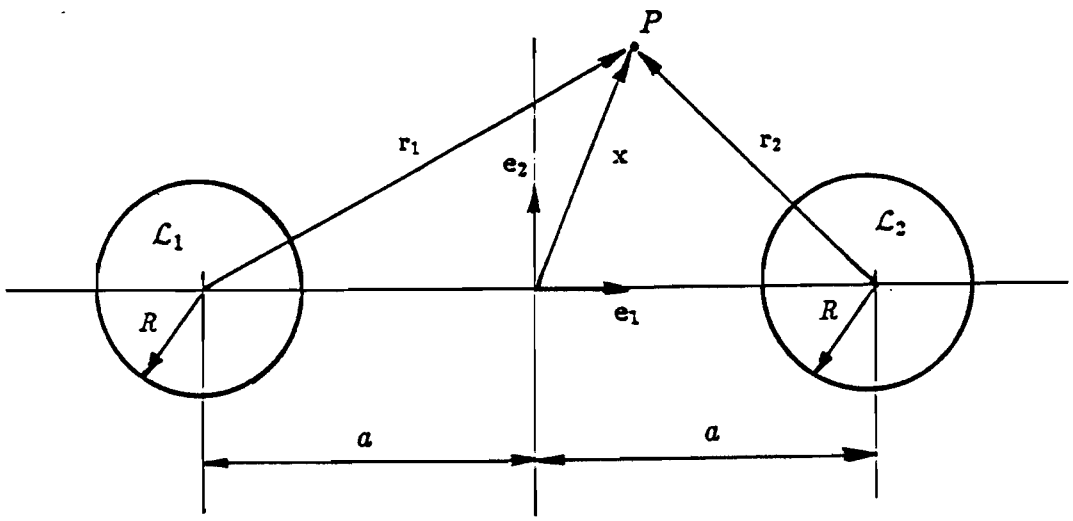

Figure 1. Cross-section of a system of two parallel rods.

The circular cross-sections of the rods have radius R and the distance between the rods is $2a$. The system is slender in so far that $R < a \ll l$ (R and a are taken to be of the same order of magnitude). An orthogonal basis $\{\mathbf{e}_1\,\mathbf{e}_2\,\mathbf{e}_3\}$ is chosen as given in Fig. 1. The deflections of the rods are in the $\mathbf{e}_1$-direction and given by

$$\mathbf{u} = \mathbf{u}^{(1)} = u^{(1)}(z)\,\mathbf{e}_1\ , \quad \text{for} \quad \mathcal{L}_1\ ; \quad \mathbf{u} = \mathbf{u}^{(2)} = u^{(2)}(z)\,\mathbf{e}_1\ , \quad \text{for} \quad \mathcal{L}_2\ . \tag{4.1}$$

From (3.7) and (3.13) we find the fields $\mathbf{B}(\mathbf{x})$ and $\psi(\mathbf{x})$ in an arbitrary point P due to the currents in $\mathcal{L}_1$ and $\mathcal{L}_2$ by simple superposition. This results in

$$\mathbf{B}(\mathbf{x}) = -\frac{\mu_0 I_0}{2\pi}\left[\left(\frac{y}{r_1^2}+\frac{y}{r_2^2}\right)\mathbf{e}_1 - \left(\frac{x+a}{r_1^2}+\frac{x-a}{r_2^2}\right)\mathbf{e}_2\right]\ , \tag{4.2}$$

and

$$\psi(\mathbf{x}) = \frac{\mu_0 I_0}{2\pi}\left[\frac{y}{r_1^2}\,u_1(z)+\frac{y}{r_2^2}\,u_2(z)\right]\ , \tag{4.3}$$

where

$$r_1^2 = (x+a)^2+y^2\ , \quad r_2^2 = (x-a)^2+y^2\ . \tag{4.4}$$

Note that in the formula (4.3) for $\psi(\mathbf{x})$ only enter the displacements of that point of $\mathcal{L}_1$ or $\mathcal{L}_2$ that has the same z-coordinate as the object point P.
For two rods

$$\partial G = \partial G_1 \cup \partial G_2 \ . \tag{4.5}$$

Introducing

$$\tilde{\psi}^{(n)} = \psi + B_k \, u_k^{(n)} \ , \qquad (n = 1,2) \ , \tag{4.6}$$

in (3.6) we obtain

$$I_0^2 \, K = -\frac{1}{2\mu_0} \sum_{n=1}^{2} \int\limits_{\partial G_n} \tilde{\psi}_{,j}^{(n)} \, [\tilde{\psi}^{(n)} \, N_j + (B_j \, N_k - B_k \, N_j) \, u_k^{(n)}] \, dS \ . \tag{4.7}$$

We may restrict ∂G_n to the region for one period, say $z \in [-l, l]$ (this is due to the periodicity of the displacement $\mathbf{u}(z)$; cf. [10], Sect. 2). With the use of (4.1)–(4.3) the right-hand side of (4.7) then becomes

$$I_0^2 \, K = -\frac{R}{2\mu_0} \sum_{n=1}^{2} \int_{-l}^{l} \int_{0}^{2\pi} \left[\tilde{\psi}^{(n)} \, \frac{\partial \tilde{\psi}^{(n)}}{\partial r} + B_\theta \, \frac{\partial \tilde{\psi}^{(n)}}{\partial y} \, u^{(n)} \right] \Big|_{\Gamma_n} d\theta \, dz \ , \tag{4.8}$$

where we have to use

$$x = (-a + R \cos\theta) \ , \quad y = R \sin\theta \ , \quad \text{for } \mathbf{x} \in \Gamma_1 \ , \tag{4.9.1}$$

and

$$x = (a + R \cos\theta) \ , \quad y = R \sin\theta \ , \quad \text{for } \mathbf{x} \in \Gamma_2 \ . \tag{4.9.2}$$

With the use of (4.2) and (4.3) the integrals in (4.8) can be evaluated. After some lengthy but elementary calculations this results in

$$I_0^2 \, K = \frac{\mu_0 I_0^2}{16\pi a^2} \, \kappa \int_{-l}^{l} [u^{(1)}(z) - u^{(2)}(z)]^2 \, dz \ , \tag{4.10}$$

where

$$\kappa = \frac{1 - 4\left(\frac{R}{2a}\right)^2 + \frac{3}{2}\left(\frac{R}{2a}\right)^4}{\left[1 - \left(\frac{R}{2a}\right)^2\right]^2} \ . \tag{4.11}$$

For the elastic energy for one period of the system we find the classical expression for the energy in bending

$$W = \tfrac{1}{2} E I \int_{-l}^{l} \left\{ \left[\frac{d^2 u^{(1)}}{dz^2}(z) \right]^2 + \left[\frac{d^2 u^{(2)}}{dz^2}(z) \right]^2 \right\} dz \,, \tag{4.12}$$

where

$$I = \frac{\pi}{4} R^4 \,, \tag{4.13}$$

is the moment of inertia about the y-axis of the circular cross-section of the rod.

The displacements $u^{(1)}(z)$ and $u^{(2)}(z)$ must satisfy the support conditions

$$u^{(i)}(kl) = 0 \,, \quad \text{and} \quad u^{(i)}(z + 2kl) = u^{(i)}(z) \,, \tag{4.14}$$

for $i \in [1,2]$ and for all $k \in \mathbb{Z}$. An admissible set of displacements (containing the lowest buckling mode) is then

$$u^{(1)}(z) = A_1 \sin\left(\frac{\pi z}{l}\right) \quad ; \quad u^{(2)}(z) = A_2 \sin\left(\frac{\pi z}{l}\right) \,. \tag{4.15}$$

Variation of J with respect to $u^{(1)}$ and $u^{(2)}$ results in the linear eigenvalue problem for I_0^2 (note that W and K are homogeneously quadratic in (A_1, A_2) and independent of I_0)

$$\frac{\partial W}{\partial A_i} - I_0^2 \frac{\partial K}{\partial A_i} = 0 \,, \quad i \in [1,2] \,. \tag{4.16}$$

The lowest eigenvalue of (4.16) corresponds to the buckling current I_0, which turns out to be equal to

$$I_0 = \frac{1}{\sqrt{\kappa}} \frac{\pi^3 a R^2}{l^2} \sqrt{\frac{E}{\mu_0}} \,. \tag{4.17}$$

We have compared this value with the corresponding values from the variational method and the Biot-Savart-method as can be found in Table 1. The result is displayed in Figure 2. In this graph the buckling currents according to the variational method (V.M.) and to the combined method (C.M.), both normalized with respect to the buckling current from the Biot-Savart-method, are displayed as function of a/R. This graph shows that the C.M.-value lies between the V.M.-value and the B.S.-value, or

$$I_0^{(B)} < I_0^{(C)} < I_0^{(V)} \,. \tag{4.18}$$

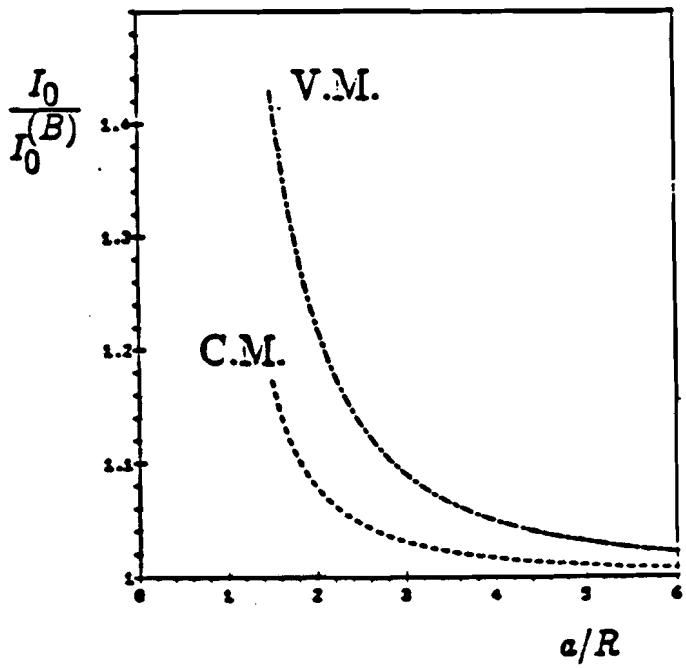

Figure 2. Comparison of the buckling values according to the variational method (V.M.), the combined method (C.M.) and the Biot-Savart method.

Hence, as could be expected, the combined method yields an improvement of the B.S.-value in the direction of the V.M.-value. However, the differences are small, and only in the region $1 < a/R < 3$ of some technical relevance. For $a/R \geq 3$ the corrections are only in the order of some few percents.

We can easily generalize the above method to sets of n $(n \geq 2)$ parallel rods. To see this more clearly it is better to write (4.10) as

$$I_0^2 K = \frac{\mu_0 I_0^2 \kappa}{8\pi} \left\{ \left(\frac{1}{2a}\right)^2 \int_{-l}^{l} [u^{(1)}(z) - u^{(2)}(z)]^2 \, dz \right.$$

$$\left. + \left(\frac{1}{2a}\right)^2 \int_{-l}^{l} [u^{(2)}(z) - u^{(1)}(z)]^2 \, dz \right\} , \tag{4.19}$$

where the first and second integral should, in principle, be performed over $\mathcal{L}_1$ and over $\mathcal{L}_2$, respectively. Moreover, it should be noted that $2a$ is the distance between the two rods.

The generalization to n rods is then straight-forward and yields

$$I_0^2 K = \frac{\mu_0 I_0^2 \kappa}{32\pi a^2} \sum_{i=1}^{n} \sum_{\substack{j=1 \\ j \neq i}}^{n} \frac{1}{(j-i)^2} \int_{-l}^{l} [u^{(i)}(z) - u^{(j)}(z)]^2 \, dz \, . \tag{4.20}$$

This formula can also be applied to more complex structures such as helical or spiral conductors. Then, n denotes the number of turns of the structures and $2a$ is the distance between two subsequent turns. These cases will be discussed in the next two sections.

5. Helical conductors

5.1. General description

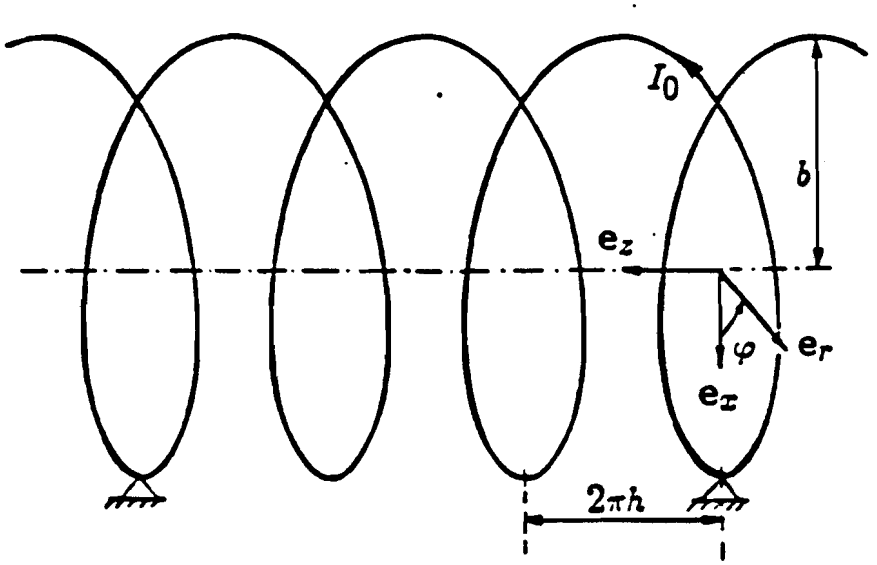

Figure 3. The helical conductor.

Let us consider a conductor in the form of a cylindrical helix (see Fig. 3). The radius of the helix is b and the (constant) pitch is h. For the distance $2a$ between two turns we then have $2a = 2\pi h$. For a slender helix $\pi h \ll b$. In the undeformed configuration a point on the central line of the helix is given by its position vector

$$\mathbf{X} = \mathbf{X}(\varphi) = b\cos\varphi\mathbf{e}_x + b\sin\varphi\mathbf{e}_y + h\varphi\mathbf{e}_z = b\mathbf{e}_r + h\varphi\mathbf{e}_z\ . \tag{5.1}$$

We shall consider both finite helices of n turns (in this case $\varphi \in [0, 2\pi n]$) as well as infinite ones ($\varphi \in [-\infty, \infty)$ then). In the first case the helix is simply supported in its end points, whereas in the latter case the helix is periodically supported in the points given by $\varphi = 0$, $\varphi = \pm 2\pi n$, $\varphi = \pm 4\pi n$, etc. The cross- section of the conductor is circular, radius R ($R < \pi h \ll b$). The total current I_0 running through the conductor is prescribed.

Since the pitch angle α is very small ($\alpha \approx b/h \ll 1$) we assume the displacement in buckling in the axial or z-direction, i.e.

$$\mathbf{u} = u(\varphi)\mathbf{e}_z\ . \tag{5.2}$$

Here, $u(\varphi)$ is the displacement of the central line of the helical conductor, causing besides a bending also a torsion of the helix. We denote the torsion angle by $\beta(\varphi)$. This torsion has no influence on the value of the integral K, it only enters the elastic energy W. By variation of W with respect to β we can obtain a relation expressing $\beta(\varphi)$ in terms of $u(\varphi)$.

For the determination of the buckling current we need expressions for the integrals K and

W. The basic idea for the calculation of K is completely analogous to the one underlying the derivation of (4.10). For a finite helix of n turns, this brings us to the following expression for K, (we have to replace a $\rightarrow \pi h$, here)

$$K = \frac{\mu_0 \kappa}{32\pi^3 h^2} \sum_{i=1}^{n} \sum_{\substack{j=1 \\ j \neq i}}^{n} \frac{1}{(j-i)^2} \int_{\mathcal{L}_i} [u^{(i)}(\varphi) - u^{(j)}(\varphi)]^2 \, b d\varphi \,, \tag{5.3}$$

where $\mathcal{L}_i$ stands for the traject

$$\mathcal{L}_i := \{\varphi \mid 2(i-1)\pi \leq \varphi < 2i\pi\} \,. \tag{5.4}$$

Moreover, for $\varphi \in \mathcal{L}_i$

$$u^{(i)} = u(\varphi) \,, \quad \text{and} \quad u^{(j)} = u(\varphi + 2(j-i)\pi) \,. \tag{5.5}$$

For the elastic energy W we use the classical expression for a slender curved beam (of circular cross-section)

$$W = \frac{EI}{2b^4} \int_{\mathcal{L}} (u'' - b\beta)^2 \, b d\varphi + \frac{GI_p}{2b^4} \int_{\mathcal{L}} (u' + b\beta')^2 \, b d\varphi =$$

$$= \frac{\pi E R^4}{8b^3} \int_{\mathcal{L}} \{(u'' - b\beta)^2 + \frac{1}{(1+\nu)} (u' + b\beta')^2\} \, d\varphi \,, \tag{5.6}$$

where we have used $I_p = 2I = \pi R^4/2$, and $G = E/2(1+\nu)$, ν denoting Poisson's modulus, while $\mathcal{L}$ stands for the total length of the helix, i.e.

$$\mathcal{L} = \sum_{i=1}^{n} \mathcal{L}_i \,. \tag{5.7}$$

As a first application we consider in the next subsection the infinite helix, followed by calculations of the buckling current for finite helices in Subsection 5.3.

5.2. The infinite helix

For the infinite helix with periodic supports over n turns, we choose for the buckling displacement field (corresponding to the lowest buckling mode)

$$u(\varphi) = A \, \sin\left(\frac{\varphi}{2n}\right) \,. \tag{5.8}$$

Note that this field satisfies the support conditions and the periodicity requirements ($k \in \mathbb{Z}$)

$$u(2\pi nk) = 0 \,, \quad \text{and} \quad u(\varphi + 4\pi nk) = u(\varphi) \,, \tag{5.9}$$

respectively. Due to the above periodicity we may restrict the value of K for an infinite helix to that for one full period (say $\varphi \in [0, 4\pi n]$). According to (5.3) we then obtain

$$K = \frac{\mu_0 \kappa b}{32\pi^3 h^2} \sum_{i=1}^{2n} \sum_{\substack{j=-\infty \\ j\neq i}}^{\infty} \frac{1}{(j-i)^2} \int_{\mathcal{L}_i} [u(\varphi) - u(\varphi + 2(j-i)\,\pi)]^2 \, d\varphi =$$

$$= \frac{\mu_0 \kappa b}{32\pi^3 h^2} \sum_{k=1}^{\infty} \frac{A^2}{k^2} \int_0^{4\pi n} \left\{ \left[\sin\left(\frac{\varphi}{2n}\right) - \sin\left(\frac{\varphi}{2n} + \frac{\pi k}{n}\right) \right]^2 \right.$$

$$\left. + \left[\sin\left(\frac{\varphi}{2n}\right) - \sin\left(\frac{\varphi}{2n} - \frac{\pi k}{n}\right) \right]^2 \right\} d\varphi =$$

$$= \frac{\mu_0 \kappa b n}{4\pi^2 h^2} A^2 \sum_{k=1}^{\infty} \frac{1}{k^2} \left(1 - \cos\frac{\pi k}{n}\right) = \frac{\mu_0 \kappa b}{8h^2} \left(1 - \frac{1}{2n}\right) A^2 \,. \tag{5.10}$$

Apart from the factor κ, this result corresponds with the K-value as found in a different way in [13], Eq. (25).
In accordance with (5.8) we assume the torsion angle $\beta(\varphi)$ of the form

$$\beta(\varphi) = \frac{1}{b} B \sin\left(\frac{\varphi}{2n}\right) \,, \tag{5.11}$$

Substitution of (5.8) and (5.11) into (5.6) yields for the elastic energy of one full period

$$W = \frac{\pi E R^4}{8b^3} \int_0^{4\pi n} \left\{ \left(\frac{A}{4n^2} + B\right)^2 \sin^2\left(\frac{\varphi}{2n}\right) + \frac{1}{4(1+\nu)\,n^2} (A+B)^2 \cos^2\left(\frac{\varphi}{2n}\right) \right\} d\varphi$$

$$= \frac{n\pi^2 E R^4}{4b^3} \left\{ \left(\frac{A}{4n^2} + B\right)^2 + \frac{1}{4(1+\nu)\,n^2} (A+B)^2 \right\} . \tag{5.12}$$

Since the first variation of J must be zero and because K is independent of β (or B) it follows that $\partial W / \partial B = 0$, yielding

$$B = -\frac{(2+\nu)}{4(1+\nu)\,n^2 + 1} A \,, \tag{5.13}$$

and with this

$$W = \frac{n\pi^2 E R^4}{4b^3} \frac{(4n^2-1)^2 A^2}{16n^4[4(1+\nu)\,n^2 + 1]} = \frac{\pi^2 E R^4 A^2}{16(1+\nu)\,n\,b^3} (1 + O(n^{-2})) \,. \tag{5.14}$$

We note that the contribution to W of the $O(n^{-2})$-term in the right-hand side of (5.14) is rather small; even for $n = 2$ it is less than 18% whereas for $n \geq 5$ it is less than 3%. Since, in practice, we are only interested in larger values of n (say $n \geq 5$) we may neglect the $O(n^{-2})$-term in (5.14). Inspection shows us that the remaining result for W is only due to the term with u' in (5.6). This leads us to the conclusion that, for $n \geq 5$, we may approximate the elastic energy by

$$W = \frac{\pi E R^4}{8(1+\nu)\,b^3} \int_{\mathcal{L}} [u'(\varphi)]^2\, d\varphi\ . \tag{5.15}$$

In the next section we shall check in how far this result also holds for a *finite* helical conductor.

With use of (5.10) and (5.14) in $J = -W + I_0^2 K$ (see (3.5)) we find from

$$\delta J = 0 \quad \Longrightarrow \quad \frac{\partial J}{\partial A} = 0\ , \tag{5.16}$$

the following relation for the buckling current

$$I_0 = \frac{\pi h R^2}{b^2} \sqrt{\frac{N(n)}{(2n-1)\,\kappa}\ \frac{E}{(1+\nu)\,\mu_0}}\ , \tag{5.17}$$

where

$$N(n) = \left(1 - \frac{1}{4n^2}\right)^2 \Big/ \left[1 + \frac{1}{4(1+\nu)\,n^2}\right] = 1 + O(n^{-2})\ . \tag{5.18}$$

Apart from the factor κ this result corresponds with that of [13]. According to its definition above N depends on ν, however, only in a very weak sense. For ν running from 0 to 0.5 the value of N changes less than 2%.

From (5.18) we conclude that I_0 is proportional to

$$\frac{\pi h R^2}{b^2} \sqrt{\frac{E}{\mu_0}}$$

as found in all systems considered thus far (see Table 1; $\pi h \leftrightarrow a$, $b \leftrightarrow l$) and, furthermore, that for the helix the buckling current is proportional to $n^{-1/2}$ for large values of n.

5.3. The finite helix

Let us consider a finite helix (as described in Section 5.1) of n turns, hence, with φ running from $\varphi = 0$ to $2\pi n$. For the evaluation of K and W we have to select a representation for the displacement field $u(\varphi)$. Due to the finiteness of the helix this representation is no longer as simple as it was in the preceding section. Here, we shall construct in two different ways a representation for $u(\varphi)$.

i) A representation in a series of sine-functions according to (we assume the first buckling mode to be symmetric about $\varphi = \pi n$)

$$u(\varphi) = \sum_{k=1}^{N} A_k\ \sin\left(\frac{(2k-1)\,\varphi}{2n}\right)\ , \tag{5.19}$$

ii) A representation in splines. For this we divide each winding in K_1 parts and we approximate $u(\varphi)$ over each part by a third order polynomial in φ. In the knots between two parts we require continuity in $u(\varphi)$ and in its first and second derivative.

We start with the evaluation of approach i). In analogy with (5.19) we choose for the torsion angle

$$b\beta(\varphi) = \sum_{k=1}^{N} B_k \sin\left(\frac{(2k-1)\varphi}{2n}\right) . \tag{5.20}$$

Substitution of (5.19) and (5.20) into the expression for the elastic energy according to (5.6) leads us to

$$W = \frac{\pi ER^4}{8b^3(1+\nu)} \int_0^{4\pi n} \{\Big[\sum_k \left(\frac{2k-1}{2n}\right)^2 (A_k + B_k) \cos\left(\frac{(2k-1)\varphi}{2n}\right)\Big]^2$$

$$+(1+\nu)\Big[\sum_k \left(\frac{(2k-1)^2}{4n^2} A_k + B_k\right) \sin\left(\frac{(2k-1)\varphi}{2n}\right)\Big]^2\} d\varphi =$$

$$= \frac{\pi^2 nER^4}{8b^3(1+\nu)} \sum_k \left\{\frac{(2k-1)^2}{4n^2} (A_k + B_k)^2 + (1+\nu)\left(\frac{(2k-1)^2}{4n^2} A_k + B_k\right)^2\right\} . \tag{5.21}$$

From

$$\frac{\partial W}{\partial B_k} = 0 , \tag{5.22}$$

we obtain

$$B_k = -\frac{(2+\nu)(2k-1)^2}{[4(1+\nu)n^2 + (2k-1)^2]} A_k , \tag{5.23}$$

yielding, after substitution in (5.21)

$$W = \frac{\pi ER^4}{8b^3(1+\nu)} \sum_k \omega_k A_k^2 , \tag{5.24}$$

with

$$\omega_k = \frac{\pi}{4n} (2k-1)^2 \left\{1 + \frac{(1+\nu)(2k-1)^2}{4n^2} - \frac{(2+\nu)^2 (2k-1)^2}{[4(1+\nu)n^2 + (2k-1)^2]}\right\} . \tag{5.25}$$

From (5.24) we conclude that with respect to the elastic energy W the A_k-modes are uncoupled.

For the magnetic K-integral (5.3) we obtain (with $m = j - i$)

$$K = \frac{\mu_0 \kappa b}{32\pi^3 h^2} \sum_{i=1}^{n} \sum_{\substack{m=-(i-1) \\ m \neq 0}}^{n-i} \frac{1}{m^2} \int_{\mathcal{L}_i} \Big\{ \sum_k A_k \Big[\sin\Big(\frac{(2k-1)\varphi}{2n}\Big)$$

$$- \sin\Big(\frac{(2k-1)\varphi}{2n} + \frac{(2k-1)\pi m}{n}\Big)\Big]\Big\}^2 d\varphi =$$

$$= \frac{\mu_0 \kappa b}{16\pi^3 h^2} \sum_{m=1}^{n-1} \frac{1}{m^2} \int_0^{2\pi(n-m)} \Big[\sum_k A_k \Big\{ \sin\Big(\frac{(2k-1)\varphi}{2n}\Big)$$

$$- \sin\Big(\frac{(2k-1)\varphi}{2n} + \frac{(2k-1)\pi m}{n}\Big)\Big\}\Big]^2 d\varphi$$

$$= \frac{\mu_0 \kappa b}{16\pi^3 h^2} \sum_{k,l=1}^{N} k_{kl} A_k A_l \,, \tag{5.26}$$

with

$$k_{kl} = \sum_{m=1}^{n-1} \frac{2n}{m^2} \Big[\frac{\pi}{n}(n-m) - \frac{1}{(2k-1)} \sin\Big(\frac{(2k-1)\pi m}{n}\Big)\Big] \sin^2\Big(\frac{(2k-1)\pi m}{2n}\Big) \,, \quad \text{if} \quad k = l \,,$$

$$k_{kl} = -\sum_{m=1}^{n-1} \frac{2n}{m^2} \Big[\frac{1}{(k+l-1)} \sin\Big(\frac{(k+l-1)\pi m}{n}\Big) + \frac{1}{(k-l)} \sin\Big(\frac{(k-l)\pi m}{n}\Big)\Big]$$

$$\sin\Big(\frac{(2k-1)\pi m}{2n}\Big) \sin\Big(\frac{(2l-1)\pi m}{2n}\Big) \,, \quad \text{if} \quad k \neq l \,. \tag{5.27}$$

With (5.24) and (5.26) we obtain from (3.5)

$$J = -\frac{\pi E R^4}{8b^3(1+\nu)} \Big\{ \sum_{k=1}^{N} \omega_k A_k^2 - \lambda \sum_{k,l=1}^{N} k_{kl} A_k A_l \Big\} \,, \tag{5.28}$$

where

$$\lambda = \frac{\kappa b^4}{2\pi^4 h^2 R^4} \frac{(1+\nu)\mu_0}{E} I_0^2 \,. \tag{5.29}$$

Variation of J with respect to A_k yields the lineair eigenvalue problem

$$\omega_k A_k - \lambda \sum_{l=1}^{N} k_{kl} A_l = 0 \,, \quad k = 1, 2, \ldots, N \,. \tag{5.30}$$

This problem is solved numerically and from the thus obtained lowest eigenvalue λ the buckling current can be calculated. The eigenvalue λ is independent of all system parameters except for the number of turns n (and also, but only in a very weak sense, except for ν). Hence $\lambda = \lambda(n)$, and from (5.29) it follows that

$$I_0 = \sqrt{\frac{2\pi^2\,\lambda(n)}{(1+\nu)\,\kappa}}\;\frac{\pi h R^2}{b^2}\;\sqrt{\frac{E}{\mu_0}}\;, \tag{5.31}$$

a result which is in form identical to all the other results listed in Table 1 (see also (5.17)).

ii) For the spline representation we first define a traject l_k ($l_k \subset \mathcal{L}$) by

$$l_k = \left\{\varphi \mid \frac{2\pi}{K_1}\,(k-1) < \varphi < \frac{2\pi}{K_1}\,k\right\}\,, \tag{5.32}$$

for $k \in [1, N]$, where $N = nK_1$, the total number of trajects (K_1 is the number of trajects per winding). We introduce local coordinates θ_k ($\theta_k \in (0,1)$) by

$$\forall_{\varphi\in l_k} \quad \varphi = \frac{2\pi}{K_1}\,(k-1+\theta_k)\,. \tag{5.33}$$

Let $w_k = w_k(\theta_k)$ be the spline approximation for $u(\varphi)$ for $\varphi \in l_k$. If w_k is known then w_{k+1} is found by the relation (from now on we write θ in stead of θ_k)

$$w_{k+1}(\theta) = w_k(1+\theta) + d_{k+1}\,\theta^3\,. \tag{5.34}$$

This definition of w_{k+1} guarantees the continuity of $u(\varphi)$, $u'(\varphi)$ and $u''(\varphi)$ in the knots $\varphi = 2\pi k/K_1$. The support conditions in $\varphi = 0$, reading $u(0) = u''(0) = 0$ (simply supported), are satisfied by taking

$$w_1(\theta) = b_1\,\theta + d_1\,\theta^3\,. \tag{5.35}$$

An iterative scheme based upon (5.34) and (5.35) yields the following general formula for w_k

$$\forall_{k\in[1,N]} \quad w_k(\theta) = (k-1+\theta)\,b_1 + \sum_{l=1}^{k}(k-l+\theta)^3\,d_l\,. \tag{5.36}$$

The support conditions in the end point $\varphi = 2\pi n$, knowing $u(2\pi n) = u''(2\pi n) = 0$, are satisfied by taking

$$b_1 = -\frac{1}{N}\sum_{l=1}^{N-1}(N+2-l)\,(N+1-l)\,(N-l)\,d_l\,, \tag{5.37.1}$$

and

$$d_N = -\sum_{l=1}^{N-1}(N+1-l)\,d_l\,. \tag{5.37.2}$$

Thus, there remain the $(N-1)$ unknown coefficients $d_1, d_2, \ldots, d_{N-1}$, which must be determined from

$$\delta J = 0 \quad \Longrightarrow \quad \frac{\partial J}{\partial d_i} = 0 \,, \quad i \in [1, N-1] \,. \tag{5.38}$$

However, before we can calculate δJ we first have to express K and W in terms of d_i. The procedure in which this is done is quite analogous to the preceding one for the sine-representation, although the arithmetics are more cumbersome here. In order to diminish these calculations we have used for W the reduced formula (5.15).
Based on the results of the preceding section we expected that this would give a fairly good approximation for not too small n. In how far this is true (or not) will be discussed in the next section. We here refrain from giving the further details of the evaluation of this spline representation. We only say that it amounts in a lineair eigenvalue problem of more or less the same type as (5.30), but, now, the matrix derived from $\partial W/\partial A_k$ is not diagonal. Thus, we here arrive at (to be compared with (5.30))

$$\sum_{l=1}^{N} \{w_{kl}\, A_l - \lambda\, k_{kl}\, A_l\} = 0 \,, \quad k = 1, 2, \ldots, N \,. \tag{5.39}$$

Again this eigenvalue problem is solved numerically. However, since the number N in this case becomes much higher than for the first case, the numerical calculations took much more time in the latter case. We return to this subject in the next section in which the explicit numerical results are presented.

5.4. Results

The lowest eigenvalues λ of the lineair eigenvalue problems derived in the preceding section are calculated numerically for a set of numbers n running from 2 to 15. We have performed these calculations for the following cases

i) eq. (5.30); i.e. the sine-representation using the full expression for the elastic energy W;

ii) the sine-representation using the reduced expression (5.15) for W;

iii) eq. (5.39); i.e. the spline-representation based on the reduced formula (5.15) for W.

In (i) we have used $\nu = 0$; the other two cases are independent of ν. In Section 5.2, however, we already showed that the influence on λ of ν is very small. The results of our calculations are presented in Table 2 and displayed graphically in Fig. 4.

Table 2.

The lowest eigenvalues λ of (5.30) or (5.39) for a set of numbers n. Case (i) eq. (5.30); (ii) eq. (5.30) with reduced W; (iii) eq. (5.39); iv) $\lambda = 1/(4\pi n)$.

n	case	2	3	4	5	6	7	8	9	10	11	12	13	14	15
$\lambda * 10^2$	(i)	3.87	2.71	2.05	1.62	1.34	1.13	.983	.866	.773	.698	.636	.584	.539	.501
	(ii)	12.50	4.26	2.64	1.92	1.50	1.23	1.05	.911	.805	.721	.654	.598	.550	.510
	(iii)	12.50	4.26	2.64	1.91	1.50	1.23	1.05	.911	.805	.721	.654	.598	.550	.510
	(iv)	3.98	2.65	1.99	1.59	1.33	1.14	.995	.884	.796	.723	.663	.612	.568	.531

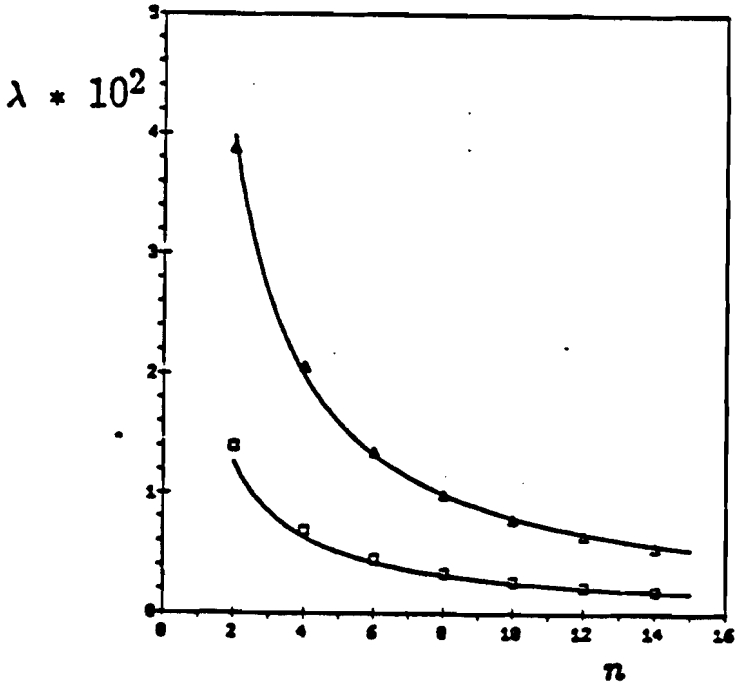

Figure 4. Buckling values for finite helices ($\triangle$; line according to (5.41)) and for infinite helices ($\square$; line according to $\lambda = 1/4\pi^2 n$) as functions of n.

From a comparison of the results for i), ii) and iii) we learn firstly that the results due to the sine-series (case ii)) and those of the spline-representation agree with each other. However, for case ii) the number N in the expansion (5.19) needed to obtain this result was equal to $(n+2)$, whereas for case iii) we had to take $K_1 \geq 3$, yielding $N \geq 3n$, to obtain convergence. The latter number becomes for large n much higher than $(n+2)$. Since N is also the order of the lineair systems (5.30) or (5.39) from which the eigenvalue λ must be calculated the calculation time for the spline-case is much longer, especially for larger n, than the one used for the sine-expansion. Moreover, also the analytical derivations are much simpler in the first than in the second case (even for the reduced elastic energy). Therefore, we conclude that the approach based on (5.19) is simple and efficient, and should be preferred above the splines representation.

Secondly, we compare the results of ii) or iii) with the more precize results of i). We see that as expected the differences between the two results decrease with increasing n. So is for $n = 5$ the relative difference still as large as 18.5%, whereas for $n = 7$ it is 9% and for $n > 9$ it is less than 5%. Still, despite this convergence, we found one noteworthy difference between the cases i) and ii). This difference lies in the buckling modes, more specifically in the values of the coefficients A_k of the eigenvector. In case ii) only the first two or three coefficients A_k submitted essentially to the determination of the buckling value; all remaining coefficients A_k could just as well have been taking zero. Hence, in this case the final value for the buckling current was already found for $N = 3$. On the other hand, in case i) the following pecularity was observed: again the first two coefficients A_1 and A_2 were dominant and it looks as if convergence was reached for $N = 3$ or 4, but for $N = n$ a sudden extra jump in λ (small but apparent) occurs. Calculation of the eigenvectors showed us that this jump was due to

the fact that now, in contrast to ii), the coefficients A_n and A_{n+1} were no longer negligible with respect to A_1 or A_2. As a consequence, complete convergence was found here only for $N \geq n+2$. As an example let us consider the case $n = 8$. For this case, we found for the normalized eigenvector

$$A_1 = -.94\ ,\quad A_2 = .25\ ,\quad A_3 = .02\ ,\quad A_8 = .21\ ,\quad A_9 = .15\ . \tag{5.40}$$

while all remaining coefficients are less than 10^{-2}. The coefficients A_8 and A_9 could only be found by using the complete version of the elastic energy; for case ii) all A_k from $k = 4$ on were less than 10^{-2}. Results analogous to (5.40) were also found for other values of n. From this we conclude that the buckling mode for helix constists of (i) a global part (represented by A_1 and A_2), and (ii) a local part on the scale of one winding (represented by A_n and A_{n+1}). The latter part must be due to the direct interaction between two adjacent windings. Although this effect with regard to the buckling mode is very striking, the influence on the buckling value itself is rather small (only a few percent).

One more comparison can be made on the hand of Table 2 or Fig. 4. We can compare the values of λ according to i) with the values of $(1/4\pi n)$ as listed in row (iv) of Table 2 (see also the line in Fig. 4). We see a good agreement between these two sets of values: nowhere for n between 2 and 15 the relative difference exceeds 5%. Hence, for practical purposes it seems allowed to use for the buckling value λ the very simple formula

$$\lambda = \frac{1}{4\pi n}\ . \tag{5.41}$$

For the buckling current of a finite simply supported helix use of this formula in (5.31) yields

$$I_0 = \frac{\pi h R^2}{b^2}\sqrt{\frac{\pi}{2n\kappa}\,\frac{E}{(1+\nu)\mu_0}}\ . \tag{5.42}$$

Comparing this result with the analogous result for an infinite helix, i.e. (5.17), we conclude that in both cases the buckling current I_0 is proportional to $n^{-1/2}$ for large values of n. However, the buckling current for a finite helix is always (no matter how large n becomes) a factor $\sqrt{\pi}$ times the one for an infinite helix (see also Fig. 4). This result contradicts the expectation stated in the conclusions of [13] saying that it is reasonable to assume that in case n is large enough the formula for the buckling current for the infinite helix also governs (in good approximation) the buckling of a finite helix of n turns. For the case of the infinite helix we separated one complete period ($\mathcal{L}^-$), i.e. $\varphi \in (0, 4\pi n)$, from the remaining part of the helix ($\mathcal{L}^+$). The statement in [13] was based on the assumption that the influence of the current in $\mathcal{L}^+$ on the forces in $\mathcal{L}^-$ becomes smaller for increasing n, and practically was restricted to a close neighbourhood of the endpoints of $\mathcal{L}^-$. If this is true, the influence of $\mathcal{L}^+$ on the buckling value diminishes and noninterference between $\mathcal{L}^-$ and $\mathcal{L}^+$ is attained for $n \to \infty$. However, the results of this section reveal that even for exceedingly large values of n the remote parts of the infinite helix remain to interfere with the inner part $\mathcal{L}^-$. Hence, the replacement of the finite helix by an infinite one, in order to get an easier problem, is not allowed.

6. Spiral conductor

6.1. General description

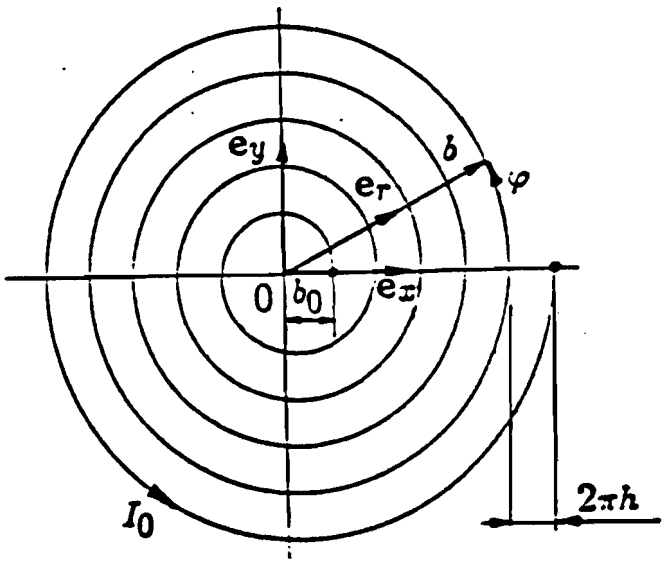

Figure 5. The flat spiral conductor.

In this section we consider a conductor in the form of a flat spiral lying in the $x - y$-plane (see Fig. 5). In the undeformed configuration a point on the central line of the spiral is given by its position vector

$$\mathbf{X} = \mathbf{X}(\varphi) = b(\varphi)\ \cos\varphi\,\mathbf{e}_x + b(\varphi)\ \sin\varphi\,\mathbf{e}_y = b(\varphi)\,\mathbf{e}_r\ , \tag{6.1}$$

with

$$b(\varphi) = b_0 + h\varphi\ ,\quad \text{for}\ \ 0 \le \varphi \le 2\pi n\ , \tag{6.2}$$

where b_0 is the radius in the begin point of the spiral, $2\pi h$ is the distance between two adjacent turns ($a = \pi h$) and n is the number of turns. The cross-section of the conductor is circular, radius R. The system is called slender if

$$\forall_{\varphi\in[0,2\pi n]}\quad \frac{R}{b(\varphi)} < \frac{\pi h}{b(\varphi)} \ll 1\ . \tag{6.3}$$

The spiral is simply supported in begin and end point. The total current I_0 running through the conductor is prescribed.

We assume that the coil buckles in its plane and that the pertinent displacement is given by (in polar coordinates)

$$\mathbf{u} = \mathbf{u}(\varphi) = u(\varphi)\,\mathbf{e}_r + v(\varphi)\,\mathbf{e}_\varphi\ . \tag{6.4}$$

The spiral is taken inextensible, yielding

$$u(\varphi) + v'(\varphi) = 0 \ , \quad \left(' = \frac{d}{d\varphi}\right) . \tag{6.5}$$

The expression for the K-integral is completely analogous to the one of the preceding chapter according to (5.3)–(5.5), however, we must realize that in (5.3) $b = b(\varphi)$ now. Note that in this expression only the radial displacement $u(\varphi)$ turns up. For an inextensible curved (almost circular) beam the elastic energy due to in-plane bending is taken equal to

$$W = \tfrac{1}{2} EI \int_0^{2\pi n} \frac{1}{b^3(\varphi)} \left[u''(\varphi) + u(\varphi)\right]^2 d\varphi \ , \tag{6.6}$$

where

$$EI = \frac{\pi}{4} ER^4 \ , \tag{6.7}$$

is the bending stiffness of a beam of circular cross-section (actually, the precize formula for W is somewhat more complex, but the extra terms are small of the order $O(h/b)$ with respect to the main term given in (6.6)).

6.2. Determination of the buckling current

Just as in the preceding section we have used here for the evaluation of K and W two different kinds of representations for $u(\varphi)$, namely, firstly a series of sine-functions and secondly a spline approximation. Again the approach via splines was rather cumbersome, using an extensive amount of computer time. Therefore, we restrict ourselves here to a description of the sine-approach only. Since, in contrast to the helix, the spiral is not symmetric about the midpoint $\varphi = \pi n$, we have to use here a complete series, that is

$$u(\varphi) = \sum_{k=1}^{N} A_k \sin\left(\frac{k\varphi}{2n}\right) . \tag{6.9}$$

Use of (6.9) in (6.6) yields

$$\begin{aligned} W &= \tfrac{1}{2} EI \int_0^{2\pi n} \frac{1}{b^3(\varphi)} \left[\sum_k \left(1 - \frac{k^2}{4n^2}\right) A_k \sin\left(\frac{k\varphi}{2n}\right)\right]^2 d\varphi = \\ &= \frac{\pi E R^4}{8 b_0^3} \sum_{k,l=1}^{N} \left(1 - \frac{k^2}{4n^2}\right)\left(1 - \frac{l^2}{4n^2}\right) I_{kl} \, A_k \, A_l \ , \end{aligned} \tag{6.10}$$

where

$$I_{kl} = \int_0^{2\pi n} \frac{1}{\beta^3(\varphi)} \sin\left(\frac{k\varphi}{2n}\right) \sin\left(\frac{l\varphi}{2n}\right) d\varphi \ , \tag{6.11}$$

and

$$\beta(\varphi) = 1 + \frac{h}{b_0}\,\varphi\,. \tag{6.12}$$

The evaluation of K is completely analogous to the one of the preceding section (see (5.26)) leading to

$$\begin{aligned} K &= \frac{\mu_0 \kappa b_0}{16\pi^3 h^2} \sum_{m=1}^{n-1} \frac{1}{m^2} \int_0^{2\pi(n-m)} \Big[1 + \frac{h}{b_0}\,(\varphi + \pi m)\Big] \cdot \Big[\sum_k A_k \{\sin\Big(\frac{k\varphi}{2n}\Big) \\ &\quad - \sin\Big(\frac{k\varphi}{2n} + \frac{k\pi m}{n}\Big)\}\Big]^2 d\varphi \\ &= \frac{\mu_0 \kappa b_0}{16\pi^3 h^2} \sum_{m=1}^{n-1} \frac{1}{m^2} \sum_{k,l=1}^{N} J_{kl}\, A_k\, A_l \sin\Big(\frac{k\pi m}{2n}\Big) \sin\Big(\frac{l\pi m}{2n}\Big)\,, \end{aligned} \tag{6.13}$$

where

$$J_{kl} = 4 \int_{\pi m}^{2\pi(n-m)} \beta(\varphi) \cos\Big(\frac{k\varphi}{2n}\Big) \cos\Big(\frac{l\varphi}{2n}\Big)\, d\varphi\,. \tag{6.14}$$

Introducing λ as (we use here $b_1 = b_0 + \pi n h$, the mean radius of the spiral, in stead of b_0 in order to weaken the influence of h on λ)

$$\lambda = \frac{\kappa b_1^4}{2\pi^4 h^2 R^4}\,\frac{\mu_0}{E}\,I_0^2\,, \tag{6.15}$$

substituting (6.10) and (6.13) into (3.5) and taking the first variation of J with respect to A_k we arrive at the lineair eigenvalue problem

$$\sum_{l=1}^{N} (w_{kl} - \lambda k_{kl})\, A_l = 0\,, \quad k = 1, 2, \ldots, N\,. \tag{6.16}$$

Explicit expressions for w_{kl} and k_{kl} can readily be read off from (6.10) and (6.13).

By a numerical solution of (6.16) the lowest eigenvalue λ can be calculated. This λ only depends on n and h and is related to the buckling current I_0 according to (6.15).

NOTE
The coefficient A_{2n} does not contribute to W nor to K. In fact this mode represents a rigid-body translation of the spiral. Therefore, in case $N \geq 2n$ we take $A_{2n} = 0$.

6.3. Results

We have calculated numerically the lowest eigenvalues of (6.16) for n running from 2 to 10

and for several values of h. The results are presented in Table 3 and displayed graphically in Figure 6.

Table 3.

The eigenvalues $\lambda * 10^2$, calculated from (6.16), for several values of n and h; the values in every second row are the outcomes of formula (6.20).

$n =$	2	3	4	5	6	7	8	9	10
$h = .050$	11.78	6.00	3.82	2.70	2.04	1.61	1.31	1.10	.96
	10.97	*5.97*	*3.88*	*2.77*	*2.11*	*1.67*	*1.37*	*1.15*	*.98*
$h = .075$	11.32	5.43	3.36	2.35	1.76	1.39	1.14	.95	.83
	9.45	*5.16*	*3.35*	*2.40*	*1.82*	*1.45*	*1.18*	*.99*	*.85*
$h = .100$	10.91	5.00	3.05	2.12	1.59	1.26	1.03	.87	.76
	8.54	*4.65*	*3.02*	*2.16*	*1.64*	*1.30*	*1.07*	*.89*	*.76*
$h = .125$	10.54	4.69	2.83	1.97	1.48	1.18	.97	.82	.72
	7.89	*4.29*	*2.79*	*1.99*	*1.52*	*1.20*	*.99*	*.83*	*.71*
$h = .150$	10.24	4.45	2.67	1.86	1.40	1.12	.92	.78	.69
	7.38	*4.02*	*2.61*	*1.87*	*1.42*	*1.13*	*.92*	*.77*	*.66*

In performing these calculations the results for the eigenvectors **A** showed us that of the coefficients A_l those for l in the neighbourhood of $2n$ where dominant. As an example let us consider the case $h = .125$ and $n = 10$. For this case we found for the (normalized) coefficients A_l,

$$A_{19} = -.657 \;\; ; \;\; A_{21} = -.513 \;\; ; \;\; A_{18} = .435 \;\; ; \;\; A_{22} = .257 \;\; ;$$

$$A_{17} = -.209 \;\; ; \;\; A_{23} = -.068 \;\; ; \;\; A_{16} = .057 \, ,$$

while all other coefficients were $\leq 10^{-2}$. Therefore, we changed the order of the summation in (6.9) in the following way

$$u(\varphi) = \sum_{k=1}^{N} \left\{ \hat{A}_{2k-1} \, \sin\left(\frac{(2n-k)}{2n}\varphi\right) + \hat{A}_{2k} \, \sin\left(\frac{(2n+k)}{2n}\varphi\right) \right\} , \tag{6.17}$$

(then $\hat{A}_1 = A_{2n-1}$, $\hat{A}_2 = A_{2n+1}$, etc.).
This reordening improved the rate of convergence substantially. In fact, we did obtain a very satisfactory convergence already for $N = 5$.

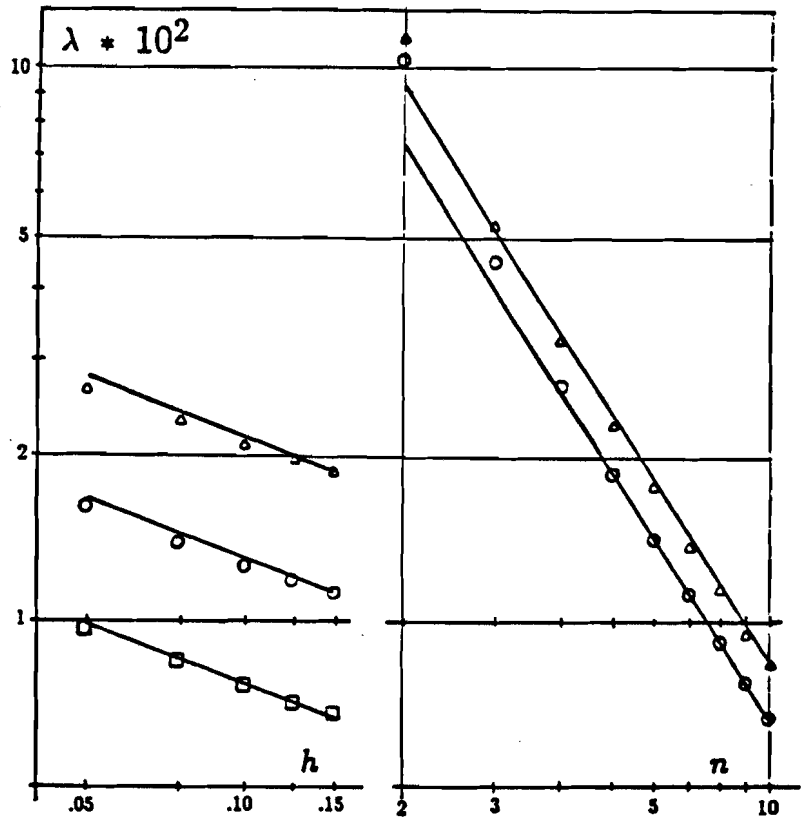

Figure 6. Buckling values for spiral conductors as function of h, for $n = 5$ ($\triangle$), $n = 7$ ($\bigcirc$) and $n = 10$ ($\square$), and as function of n for $h = .075$ ($\triangle$) and $h = .15$ ($\bigcirc$), both plotted on a double logarithmic scale.

The behaviour of λ as function of n or h is shown in the graphs of Figure 6. When plotted on a logarithmic scale this behaviour was rectilinear (in a good approximation) bot for h ($h \in [.05;\ .15]$) as for, not too small, n (for $n \geq 4$). This implies that $\lambda = \lambda(n, h)$ must be of the form

$$\lambda = A\, h^{\alpha} \left(\frac{1}{n}\right)^{\beta} . \tag{6.18}$$

By means of a least square approximation the best values for the exponentials α and β are calculated. Thus, we found

$$A = 10.55\ ,\quad \alpha = -.36\quad ;\quad \beta = 1.5\ , \tag{6.19}$$

yielding

$$\lambda = 10.55 \left(\frac{1}{h}\right)^{.36} \left(\frac{1}{n}\right)^{1.5} , \tag{6.20}$$

holding for the range $h \in [.05\ ;\ .15]$ and $n \geq 4$. The results of this formula are also listed in Table 3 (see also Figure 6). Everywhere in the given range the errors made by using (6.20)

in stead of (6.15) are less than 5%. Hence, (6.20) represents a useful empirical formula for the buckling current, which then follows from (6.15) as

$$I_0 = \frac{\pi h R^2}{b_1^2} \sqrt{\frac{2\pi^2 \lambda}{\kappa} \frac{E}{\mu_0}} . \tag{6.21}$$

We also have performed calculations for λ on basis of a spline approximation and by a discretization for the displacement field $u(\varphi)$. The obtained numerical results showed a correspondence with the results presented here, but despite of a much greater amount of computer time, the results were still less precise than those from the sine- approach. Hence, the use of a series of sines for $u(\varphi)$ turns out to be preferable here as well as it was for the helical conductor.

From the calculated values of the coefficients A_l of the eigenvector we could obtain an impression of the buckling mode. After the elimination of an apparent rigid body mode we found buckling displacement fields as shown for two cases in Figure 7. The rigid body field was eliminated by adding to the series in (6.17) an extra mode of the form $A_0 \sin \varphi$, (note that this term does not contribute to either W or K, and that $u = A_0 \sin \varphi$ in combination with $v = A_0 \cos \varphi$, and in a small (h/b) approximation, represents a rigid-body translation). The coefficient A_0 was chosen such as to minimize this rigid-body displacement. For the example $h = .125$ and $n = 10$ given in the beginning of this section this led us to a value of $A_0 = .70$.

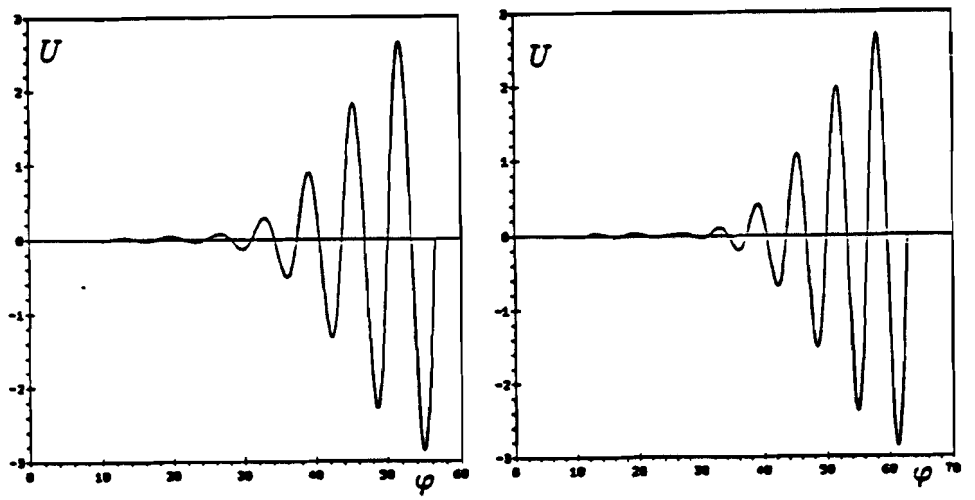

Figure 7. Buckling modes for spiral conductors for i) $h = .075$, $n = 9$, and ii) $h = .125$, $n = 10$.

The results, displayed in Figure 7 for the cases $h = .075$, $n = 9$ and $h = .125$, $n = 10$, show that the displacements in the outer coils prevail over those in the inner coils. This could be expected in virtue of the larger mechanical stiffness of the inner coils compared to the outer ones.

7. Conclusions

We have established a new method for the determination of the buckling current of a superconducting structure, which is a combination of two older methods. This so called combination method (C.M.) is so constructed as to retain the advantages of the two basical methods (i.e. a variational method (V.M.) and the Biot-Savart method (B.S.)) and, at the same time, to get rid of the associated disadvantages. This led us to a method which is both sufficiently exact for practical purposes as well as convenient to use in practice. For the example of a system of n parallel rods we have shown that the values from C.M. are in between those from V.M. and B.S. (which are already not so far apart). The solution of the system of n rods also provided us with an expression for the magnetic interaction term which could be used for helical and spiral conductors. This result, i.e. an easy manageable expression for the magnetic interaction integral occurring in our variational principle, was one of the main goals of this research. With use of this expression we have solved the buckling problem for (in)finite helical and spiral conductors (both simply supported in their end points). We recapitulate some of the main results.

i) For an infinite helix, periodically supported over n turns, we have (see (5.17))

$$I_0 = \sqrt{\frac{N(n)}{(2n-1)\,(1+\nu)\,\kappa}}\;\frac{\pi\,h\,R^2}{b^2}\;\sqrt{\frac{E}{\mu_0}}\,, \tag{7.1}$$

(where $N(n)$ and κ are numerical factors close to unity).

ii) For a finite helix of n turns ((5.31) and (5.42))

$$I_0 = \sqrt{\frac{2\pi^2\,\lambda(n)}{(1+\nu)\,\kappa}}\;\frac{\pi\,h\,R^2}{b^2}\;\sqrt{\frac{E}{\mu_0}} \approx \sqrt{\frac{\pi}{2n(1+\nu)\,\kappa}}\;\frac{\pi\,h\,R^2}{b^2}\;\sqrt{\frac{E}{\mu_0}}\,. \tag{7.2}$$

iii) For both the finite and infinite helix the buckling current I_0 is proportional to $(1/n)^{\frac{1}{2}}$ for $n \gg 1$. However, for large values of n the buckling current for the finite helix is $\sqrt{\pi}$ times the one for the infinite helix.

iv) For a (flat) spiral of n turns ((6.21))

$$I_0 = \sqrt{\frac{2\pi^2\,\lambda(n,h)}{\kappa}}\;\frac{\pi\,h\,R^2}{b^2}\;\sqrt{\frac{E}{\mu_0}}\,, \tag{7.3}$$

with λ according to (6.20), showing that $I_0 \propto (1/n)^{\frac{3}{4}}$ for $n \gg 1$.

v) In buckling the displacements of the outer coils of the spiral are dominant over those of the inner coils (which remain practically undeformed).

As a general conclusion we can state that for all cases mentioned in this paper the buckling formula is always of the same form, namely (here, l is a characteristic global measure of length, e.g. $l = \pi b$ for the helix or spiral)

$$I_0 = \Lambda \frac{a R^2}{l^2} \sqrt{\frac{E}{\mu_0}}, \tag{7.4}$$

($a = \pi h$, for helix or spiral) where the pre-factor Λ, which differs from case to case, is independent of R and l (it may depend on a and further on n and ν). Specific expressions for Λ can be red from Table 1 or the results (7.1)–(7.3) listed above. In (5.42) and (6.20) empirical formulas for Λ are given, valid for a wide range of the parameters n and λ, which are very easy for direct practical use.

In all the structures considered here the cross-section was always taken to be circular. However, for the calculation of the magnetic integral we used the Biot-Savart field as an admissible field, but in the Biot-Savart approach the current carrier is considered as a one-dimensional curve, *irrespective of the specific form of the cross-section.* Hence, since we have shown that the preciseness of the Biot-Savart method was more than acceptable, the specific form of the cross-section is, at least as far as the magnetic part of our Lagrangian concerns, not very relevant. Of course, the form of the cross-section does be of relevance for the calculation of the elastic energy.

In returning to Section 2, where we shortly outlined the variational method, and to our earlier work we recall that the most difficult part in the application of the variational method was the determination of the magnetic integral (K); the determination of the elastic energy (W) was often a straightforward (classical) problem. However, we must admit that we have considered here only pure systems, meaning that W was only coming from the current carrying structure itself. In other words, we did not include elastic stiffness of, for instance, a matrix supporting the conductor. This made it practically impossible to compare our theoretical results with experimental results, as far as they are available. There are some experimental results, a.o. from Miya et al., [6], [7], but they all apply to constructions of embedded conductors. Of course, these kind of constructions are of greater practical relevance then the pure constructions considered by us.
However, our first aim was to construct on a firm theoretical basis an expression for the magnetic interaction term (characteristic for the magnetic forces on the structure) and I think we have succeeded in this goal. Since this magnetic term is not influenced by the matrix material (nor by any other type of elastic support) this particular result remains valid for superconducting structures embedded in a matrix. We only have to recalculate the elastic energy term. This seems to me a subject for future research and, possibly, then comparison with experimental results can be made.

6. References

[1] F.C. Moon and Yih-Hsing Pao, Magnetoelastic buckling of a thin plate, ASME J. Appl. Mech. **35** (1968) 53–58.

[2] F.C. Moon, Magneto-solid mechanics (Wiley, New York, 1984).

[3] S. Chattopadhyay and F.C. Moon, Magnetoelastic buckling and vibration of a rod carrying electric current, ASME J. Appl. Mech. **42** (1975) 809–914.

[4] S. Chattopadhyay, Magnetoelastic instability of structures carrying electric current, Int. J. Solids Struct. **15** (1979) 467–477.

[5] A.A.F. van de Ven and M.J.H. Couwenberg, Magnetoelastic stability of a superconducting ring in its own field, J. Eng. Math. **20** (1986) 251–270.

[6] K. Miya and M. Uesaka, An application of finite element method to magnetomechanics of superconducting magnets for magnetic fusion reactors, Nucl. Engrg. Des. **72** (1982) 275–296.

[7] T. Takaghi, K. Miya, H. Yamada and T. Takagi, Theoretical and experimental study on the magnetomechanical behavior of superconducting helical coils for a fusion reactor, Nucl. Engrg. Des/Fus. **1** (1984) 61–71.

[8] W. Geiger and K.P. Jüngst, Buckling calculations and measurements on a technologically relevant toroidal magnet system, ASME J. Appl. Mech. **58** (1991), 167–174.

[9] P.H. van Lieshout, P.M.J. Rongen and A.A.F. van de Ven, A variational principle for magneto-elastic buckling, J. Eng. Math. **21** (1987) 227–252.

[10] P.H. van Lieshout, P.M.J. Rongen and A.A.F. van de Ven, A variational approach to magneto-elastic buckling problems for systems of ferromagnetic or superconducting beams, J. Eng. Math. **22** (1988) 143–176.

[11] P.R.J.M. Smits, P.H. van Lieshout and A.A.F. van de Ven, A variational approach to magnetoelastic buckling problems for systems of superconducting tori, J. Eng. Math. **23** (1989) 157–186.

[12] P.H. van Lieshout and A.A.F. van de Ven, A variational approach to the magnetoelastic buckling problem of an arbitrary number of superconducting beams, J. Eng. Math. **25** (1991) 353–374.

[13] A.A.F. van de Ven and P.H. van Lieshout, Buckling of superconducting structures under prescribed current, Proceedings of IUTAM-Symposium on the Mechanical Modellings of the New Electromagnetic Materials, R.K.T. Hsieh (ed.), Stockholm 1990, pp. 35–42, Elsevier, Amsterdam (1990).

[14] K. Hutter and A.A.F. van de Ven, Field Matter Interactions in Thermoelastic Solids, Lecture Notes in Physics, Vol. 88, Springer Verlag, Berlin (1978).